Scientia Iranica B (2018) 25(4), 2130–2143

Sharif University of Technology
Scientia Iranica
Transactions B: Mechanical Engineering
http://scientiairanica.sharif.edu

Numerical solution to N-S equations in the case of unsteady axisymmetric stagnation-point flow on a vertical circular cylinder with mixed convection heat transfer

R. Bayat and A.B. Rahimi*

Faculty of Engineering, Ferdowsi University of Mashhad, Mashhad, P.O. Box 91775-1111, Iran.

Received 28 August 2016; accepted 17 July 2017

KEYWORDS
Numerical solution;
Stagnation-point flow;
Vertical circular cylinder;
Mixed convection;
Entropy generation.

Abstract. The unsteady problem of impulsive stagnation-point flow on a vertical circular cylinder along with mixed convection heat transfer was solved numerically for the first time. The mentioned problem suffered from shortcomings of similarity solution techniques when encountering various physical conditions such as time-dependent states. Initially, the fluid was considered to be at rest, with a uniform temperature T_∞. At $t = 0$, this fluid starts flowing toward a vertical cylinder at the strength rate of $\bar{k}$, and the cylinder surface's temperature rises to T_w, simultaneously. The Navier-Stokes and energy equations in a cylindrical coordinate system were discretized and solved in a 2D domain using a SIMPLE-based algorithm. The solution was obtained in three cases: firstly, when cylinder's wall temperature, T_w, is constant; secondly, when T_w varies linearly along cylinder's axis; thirdly, when it has parabolic variations. Considering a sample case of incompressible flow with Re = 1 and Pr = 0.7, the results of Nusselt number, wall shear-stress, and dimensionless velocity and temperature were obtained under different states of cylinder's wall temperatures for some selected values of Grashof numbers. An entropy generation analysis for the case of constant wall temperature is performed, which is the first of its kind as conducted in this paper.

© 2018 Sharif University of Technology. All rights reserved.

1. Introduction

The problem of stagnation-point flow and heat transfer on a plate or cylinder has always been a highly intriguing issue to study due to its various industrial applications. For example, in metal, plastic, or food products manufacturing by extrusion process, the output product is usually cooled by blowing a peripheral fluid flow. Since the cooling process affects the resistance and quality of the product, analytical modeling and evaluation of this physical event are carried out under the topic of stagnation-flow problem. By using analytical methods, particularly similarity solutions, accurate results can be obtained demonstrating flow behavior in a viscous boundary layer. However, finding the appropriate similarity variables and solving the governing differential equations of the problem are the main challenges of this approach. Besides, the solvable self-similar or semi-similar equations can be produced for only few specific boundary conditions. The history of the analytical methods studies using similarity solution techniques goes back to Hiemenz [1]. He investigated the steady two-dimensional laminar

*. *Corresponding author. Tel.: 098 5138805018*
E-mail address: rahimiab@um.ac.ir (A.B. Rahimi)

doi: 10.24200/sci.2017.4347

incompressible flow perpendicularly impinging on a flat plate and succeeded to transform governing equations into ordinary differential equations. These equations were then solved using numerical methods. Wang [2] was the first to present the solution of stagnation-point flow on a circular cylinder. This problem was for the simple case of a stationary cylinder without suction and blowing in a steady-state condition. The importance of this problem was due to the introduction of different similarity variables to cylindrical coordinate system. Based on Wang's accomplishment, Gorla [3] could obtain both velocity and temperature distributions for a cylinder with constant wall temperature and constant heat flux. He considered energy equation, used a transformation for temperature quantity, and then solved the extracted differential equations by numerical methods. Gorla [4] continued his work and solved the problem of transient state when the free stream flow has time-dependent velocity. He used the series form solution in his analysis and presented the results for some specific time-dependent functions. In his next paper, Gorla [5] assumed the cylinder with harmonic motion and obtained the results of this unsteady problem for two cases of low and high frequencies. Ramachandran et al. [6] dealt with solving the problem of normal stagnation-point flow against a vertical flat plate in the presence of buoyancy forces, causing mixed convection. Gorla [7] studied mixed convection of a vertical circular cylinder impinged by a normal stagnation-point flow. He presented a numerical solution to the equations in the case of constant or linearly variable wall temperature. Takhar et al. [8] investigated the unsteady case of this problem for any arbitrary time-dependent free-stream or cylinder velocities. They obtained numerical methods for solving their final differential equations in the cases of semi-similar and self-similar forms. Rahimi [9] used the perturbation technique to solve the problem of stagnation flow and heat transfer on a cylinder for high Reynolds numbers. In their two papers, Saleh and Rahimi [10,11] presented the similarity solution of axisymmetric stagnation-point flow and heat transfer on a moving cylinder when it has time-dependent axial velocity and uniform transpiration. Saleh and Rahimi [12,13] dealt with the same problem by considering rotational movement for the cylinder with time-dependent angular velocity. In addition, they [14] solved unaxisymmetric flow and heat transfer in the axisymmetric stagnation-point flow on a cylinder, which has simultaneous axial and rotational movements along with transpiration. The unaxisymmetry of the problem is caused by non-symmetrical transpiration around the cylinder axis. Revnic et al. [15] dealt with mixed convection heat transfer problem of a circular cylinder impinged by a normal stagnation-point flow, already mentioned by Gorla [7], and presented its numerical solution for a wider range of dimensionless numbers. Mohammadiun and Rahimi [16] were the first to introduce the similarity variables for solving stagnation-point flow and heat transfer of a compressible fluid on a stationary cylinder. Therefore, they could include the effect of the variable density in the resulting similar forms of velocity and temperature equations, which were solved simultaneously. Lok et al. [17] added the stretching or shrinking effects to the problem of mixed convection heat transfer of the axisymmetric stagnation-point flow on a cylinder, already solved by Gorla [7]. Mohammadiun et al. [18] solved the above-mentioned problem in their paper [16] for the condition of cylinder with a constant heat flux. The list goes on until the very recent years, e.g., a study by Bayat and Rahimi [19].

In all the above works, the similarity solution techniques were used. Although this method of solution has high importance from mathematical point of view, it has certain shortcomings too, especially when encountering various physical conditions such as time-dependent states. For this reason, in the present analysis and for the first time, the unsteady problem of mixed convection heat transfer from a vertical circular cylinder impinged by an impulsive axisymmetric stagnation-point flow is solved by employing numerical methods. An implicit numerical solution to Navier-Stokes and energy equations in a two-dimensional zone with appropriate boundary conditions is applied. Herein, the velocity and temperature parameters are obtained directly. It is considered that a constant-strength axisymmetric outer flow impinges on a vertical circular cylinder along with gravitational effects. The flow is considered inviscid far from the cylinder. In the region near the surface (solution domain), equations of viscous flow and energy are discretized according to the finite-difference scheme, and the resulting system of equations is solved by the well-known TDMA algorithm. The obtained results are verified through a comparison with Gorla's [3] for the specific case of $T_w = \text{const.}$ and $\text{Gr} = 0$. More data are obtained for variable T_w and non-zero Grashof numbers, too.

2. Problem formulation

Axisymmetric incompressible stagnation-point flow impinges impulsively on a vertical circular cylinder. The radius of this cylinder is a with the length of infinity and with wall temperature, T_w, in the space influenced by gravity acceleration, g. A schematic of this problem is presented in Figure 1. It is obvious that, for the upper half of the geometry (i.e., $z > 0$), the buoyancy forces are in the same direction with the flow; therefore, herein, there exists an assisting flow condition. In contrast, for $z < 0$, there is the opposing state of flow because the fluid flows downward. The flow far from

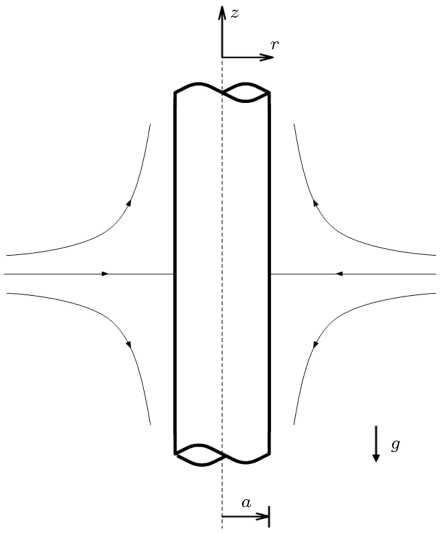

Figure 1. Schematic of axisymmetric stagnation flow on a vertical circular cylinder.

the cylinder's surface is assumed as an inviscid flow with the rate of strength, $\bar{k}$. Then, according to the axisymmetric coordinate system (r, z) in Figure 1, by referring to Wang [2], velocity components, U and W, of this free stream flow are expressed as follows:

$$\begin{cases} U = -\left(r - \frac{1}{r}\right) \\ W = 2z \end{cases} \tag{1}$$

where coordinates r and z are non-dimensionalized with radius a and velocities U and W with $a\bar{k}$.

2.1. Governing equations

Supposing the presence of an incompressible viscous flow in the axisymmetric cylindrical coordinate system, the basic time-dependent equations in terms of velocity components $u(r, z, t)$ in r-direction, $w(r, z, t)$ in z-direction, and temperature field, $T(r, z, t)$, have the following dimensionless forms:

Mass continuity:

$$\frac{\partial}{\partial r}(ru) + r\frac{\partial w}{\partial z} = 0. \tag{2}$$

Momentum equations (Navier-Stokes equations):

$$2\frac{\partial u}{\partial \tau} + u\frac{\partial u}{\partial r} + w\frac{\partial u}{\partial z} = -\frac{\partial p}{\partial r} + \frac{1}{2\mathrm{Re}}\left(\frac{\partial^2 u}{\partial r^2} + \frac{1}{r}\frac{\partial u}{\partial r} - \frac{u}{r^2} + \frac{\partial^2 u}{\partial z^2}\right), \tag{3}$$

$$2\frac{\partial w}{\partial \tau} + u\frac{\partial w}{\partial r} + w\frac{\partial w}{\partial z} = -\frac{\partial p}{\partial z} + \frac{1}{2\mathrm{Re}}\left(\frac{\partial^2 w}{\partial r^2} + \frac{1}{r}\frac{\partial w}{\partial r} + \frac{\partial^2 w}{\partial z^2}\right) + \frac{\mathrm{Gr}}{4\mathrm{Re}^2}\theta. \tag{4}$$

Velocity components u and w are non-dimensionalized with $a\bar{k}$ and pressure p with $\rho a^2\bar{k}^2$. For example, the non-dimensionalization process of Eq. (3) is shown below:

$$\frac{\partial\left(\frac{u}{a\bar{k}}\right)}{\partial(\bar{k}t)} + \left(\frac{u}{a\bar{k}}\right)\frac{\partial\left(\frac{u}{a\bar{k}}\right)}{\partial\left(\frac{r}{a}\right)} + \left(\frac{w}{a\bar{k}}\right)\frac{\partial\left(\frac{u}{a\bar{k}}\right)}{\partial\left(\frac{z}{a}\right)} = -\frac{\partial\left(\frac{p}{\rho a^2\bar{k}}\right)}{\partial\left(\frac{r}{a}\right)} + \frac{\upsilon}{a^2\bar{k}}\left[\frac{\partial^2\left(\frac{u}{a\bar{k}}\right)}{\partial\left(\frac{r}{a}\right)^2} + \frac{1}{\left(\frac{r}{a}\right)}\frac{\partial\left(\frac{u}{a\bar{k}}\right)}{\partial\left(\frac{r}{a}\right)} - \frac{\left(\frac{u}{a\bar{k}}\right)}{\left(\frac{r}{a}\right)^2} + \frac{\partial^2\left(\frac{u}{a\bar{k}}\right)}{\partial\left(\frac{z}{a}\right)^2}\right]. \tag{4-1}$$

In addition, dimensionless time, τ, and temperature, θ, have the following expressions:

$$\tau = 2\bar{k}t, \qquad \theta = \frac{T - T_\infty}{T_w - T_\infty}. \tag{5}$$

The last term in Eq. (4) is due to the presence of buoyancy forces in z-direction, which is according to the Boussinesq's approximation.

Energy equation:
In the general case of $T_w = T_w(z)$:

$$2\frac{\partial\theta}{\partial\tau} + u\frac{\partial\theta}{\partial r} + w\left(\frac{\partial\theta}{\partial z} + \frac{\frac{dT_w}{dz}}{T_w - T_\infty}\theta\right) = \frac{1}{2\mathrm{Re.Pr}}\left[\frac{\partial^2\theta}{\partial r^2} + \frac{1}{r}\frac{\partial\theta}{\partial r} + \frac{\partial^2\theta}{\partial z^2} + \frac{2\frac{dT_w}{dz}}{T_w - T_\infty}\frac{\partial\theta}{\partial z} + \frac{\frac{d^2T_w}{dz^2}}{T_w - T_\infty}\theta\right], \tag{6}$$

where the Reynolds, Prandtl, and Grashof numbers have the following definitions:

$$\mathrm{Re} = \frac{\bar{k}a^2}{2\upsilon}, \qquad \mathrm{Pr} = \frac{\upsilon}{\alpha}, \qquad \mathrm{Gr} = \frac{g\beta(T_w - T_\infty)a^3}{\upsilon^2}. \tag{7}$$

The boundary conditions of the problem with respect to the no-slip condition and $T = T_w$ on the cylinder's surface on the one side, and inlet inviscid flow with T_∞ on the other side of the domain of solution are:

$$\begin{aligned} &r = 1: && u = w = 0, \quad \text{and} \quad \theta = 1, \\ &r = R_{\max}: && u = U, \quad w = W, \quad \text{and} \quad \theta = 0. \end{aligned} \tag{8}$$

For outlet boundaries, by considering velocity field of the inviscid flow in Eq. (1), it is supposed that $u = u(r)$ and $w = z$, then we will have following conditions:

$$z = Z_{\min}, Z_{\max}: \qquad \frac{\partial u}{\partial z} = 0, \quad \frac{\partial w}{\partial z} = \frac{w}{z}. \tag{9}$$

In addition, θ is extrapolated by the two previous points as the boundary condition of the temperature at outlets.

Since unsteadiness of the problem is a consequence of impulsive motion of the free stream flow at $t = 0$, the fluid at rest (no motion) with uniform temperature, T_∞, in both fluid and cylinder's wall for $t < 0$ as initial conditions is considered. For $t \geq 0$, a sudden free stream flow, according to Eq. (1), appears, whereas the cylinder's wall temperature rises to T_w, simultaneously.

2.2. Flow characteristics

When numerical results of the velocity and temperature field are determined, Nusselt number and wall shear-stress, non-dimensionalized by $\mu\bar{k}$, can be obtained from the following relations by a forward difference approximation:

$$\mathrm{Nu} = \frac{ha}{2k} = -\frac{1}{2}\left[\frac{\partial\theta}{\partial r}\right]_{r=1}, \qquad \tau_w = \left[\frac{\partial w}{\partial r}\right]_{r=1}. \quad (10)$$

2.3. Entropy generation

The volumetric rate of local entropy generation, which arises due to the heat transfer and fluid friction losses, is given by:

$$\dot{S}'''_{\mathrm{gen}} = \frac{k}{T^2}(\nabla T)^2 + \frac{\Phi}{T}, \quad (11)$$

where ∇T represents the temperature gradient and Φ is the dissipation function. Defining entropy generation number as $N_s = a^2\dot{S}'''_{\mathrm{gen}}/k$ (normalized form of $\dot{S}'''_{\mathrm{gen}}$), entropy generation number due to heat transfer irreversibility, N_H, and entropy generation number due to fluid friction irreversibility, N_F, the above equation can be rewritten as follows:

$$N_S = N_H + N_F. \quad (12)$$

Supposing axisymmetry in the cylindrical coordinates system and $T_w = \mathrm{Const.}$, we have [20]:

$$N_H = \frac{1}{\left(\theta + \frac{1}{\gamma-1}\right)^2}\left[\left(\frac{\partial\theta}{\partial r}\right)^2 + \left(\frac{\partial\theta}{\partial z}\right)^2\right], \quad (13)$$

$$N_F = \frac{\mathrm{Br}}{\theta + \frac{1}{\gamma-1}}\left\{2\left[\left(\frac{\partial u}{\partial r}\right)^2 + \left(\frac{\partial w}{\partial z}\right)^2\right] + \left(\frac{\partial u}{\partial z} + \frac{\partial w}{\partial r}\right)^2\right\}, \quad (14)$$

where $\gamma = T_w/T_\infty$ and $\mathrm{Br} = \frac{\mu a^2\bar{k}^2}{k(T_w - T_\infty)}$ is Brinkman number.

Also, it is useful to determine the portion of the entropy generation due to heat transfer in the overall entropy generation by calculating Bejan number with the following definition:

$$\mathrm{Be} = \frac{N_H}{N_S}. \quad (15)$$

3. Method of solution

Eqs. (3), (4), and (6) under boundary conditions (8) are solved numerically using an implicit finite-difference scheme based on SIMPLE algorithm. For this purpose, a computer code in Fortran software is provided. Due to the problem's axisymmetry, a rectangular zone is chosen as a 2D domain of solution in r-z-plane which is located between $r = 1$ to $r = R_{\max}$ and $z = Z_{\min}$ to $z = Z_{\max}$ (Figure 2). This domain, typically meshed by a staggered square grid system, is shown in Figure 3. All first-order and second-order derivatives with respect to r and z are discretized using a central difference formulation. The first-order derivatives in τ are replaced by a backward difference approximation. Besides, the coefficient in the nonlinear convective terms is approximated by the known value from previous time level. As an example, discretization of u-component of velocity is presented below. Indices i and j are related to r and z, respectively:

$$2\frac{u^*_{i,j} - u^n_{i,j}}{\Delta t} + u^n_{i,j}\frac{u^*_{i+1,j} - u^*_{i-1,j}}{2\Delta r} + w^n_{i,j}\frac{u^*_{i,j+1} - u^*_{i,j-1}}{2\Delta z} = -\left(\frac{p^*_{i+1,j} - p^*_{i-1,j}}{2\Delta r}\right) + \frac{1}{2\mathrm{Re}}\left(\frac{u^*_{i-1,j} - 2u^*_{i,j} + u^*_{i+1,j}}{\Delta r^2}\right.$$

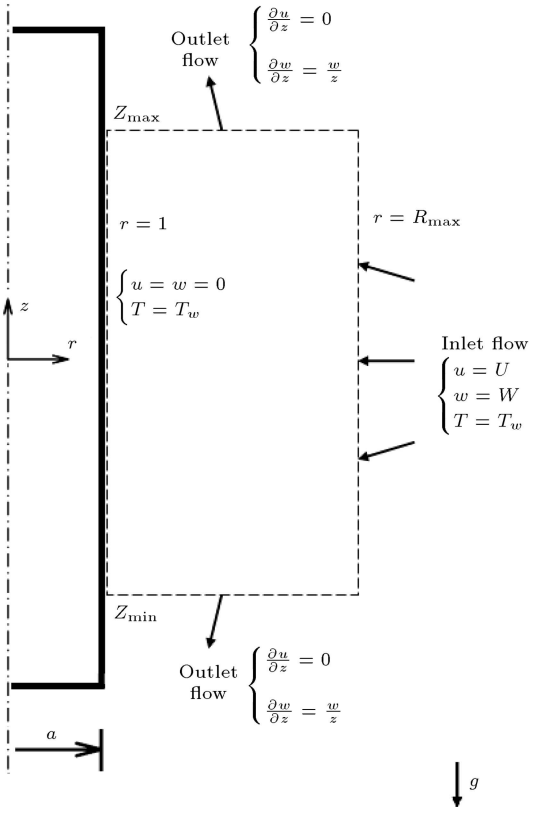

Figure 2. Illustration of the domain of the solution.

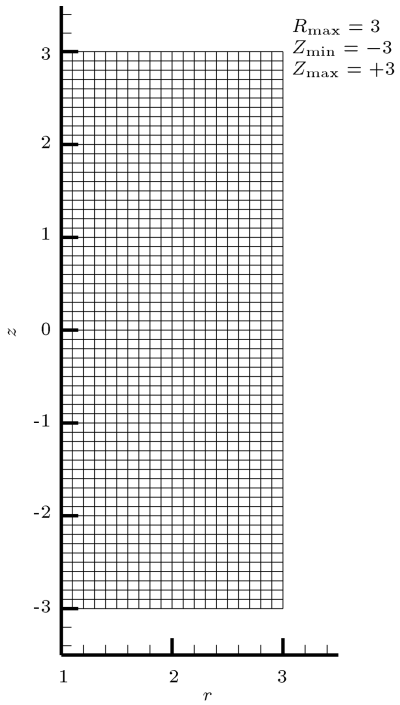

Figure 3. Sample of the meshed domain.

$$+\frac{1}{r_{i,j}}\frac{u^*_{i+1,j}-u^*_{i-1,j}}{2\Delta r}-\frac{u^*_{i,j}}{r^2_{i,j}}+\frac{u^*_{i,j-1}-2u^*_{i,j}+u^*_{i,j+1}}{\Delta z^2}\Bigg). \quad (15\text{-}1)$$

Superscript n is the value of equation parameters at a specific time. Superscript * represents equation solutions for initial guess of pressure field, p^*. Writing u based on constant j (sweeping in z-direction) gives:

$$\left(-\frac{u^n_{i,j}}{2\Delta r}-\frac{1}{2\mathrm{Re}\Delta r^2}+\frac{1}{4\mathrm{Re}r_{i,j}\Delta r}\right)u^*_{i-1,j}+\left(\frac{2}{\Delta t}+\frac{1}{\mathrm{Re}\Delta r^2}+\frac{1}{2\mathrm{Re}r^2_{i,j}}+\frac{1}{\mathrm{Re}\Delta z^2}\right)u^*_{i,j}+\left(\frac{u^n_{i,j}}{2\Delta r}-\frac{1}{2\mathrm{Re}\Delta r^2}-\frac{1}{4\mathrm{Re}r_{i,j}\Delta r}\right)u^*_{i+1,j}=\frac{2u^n_{i,j}}{\Delta t}+\frac{p^*_{i-1,j}-p^*_{i+1,j}}{2\Delta r}+\left(\frac{w^n_{i,j}}{2\Delta z}+\frac{1}{2\mathrm{Re}\Delta z^2}\right)u^*_{i,j-1}+\left(-\frac{w^n_{i,j}}{2\Delta z}+\frac{1}{2\mathrm{Re}\Delta z^2}\right)u^*_{i,j+1}. \quad (15\text{-}2)$$

Writing u based on constant I (sweeping in r-direction) gives:

Table 1. Inlet and outlet flow rates related to the solution domain with dimensions $R_{max} = 4$ and $Z_{max,min} = \pm 3$.

Step size	Q_{in}	Q_{out}	Error (%)
$\Delta r = \Delta z$=0.02	565.4867	563.7842	0.301068
$\Delta r = \Delta z$=0.03	565.4867	567.4353	0.344588
$\Delta r = \Delta z$=0.04	565.4867	563.7758	0.302554
$\Delta r = \Delta z$=0.05	565.4867	566.2092	0.127766
$\Delta r = \Delta z$=0.06	565.4867	563.8697	0.285948
$\Delta r = \Delta z$=0.075	565.4867	564.1638	0.23394
$\Delta r = \Delta z$=0.1	565.4867	564.3403	0.202728

$$\left(-\frac{w^n_{i,j}}{2\Delta z}-\frac{1}{2\mathrm{Re}\Delta z^2}\right)u^*_{i,j-1}+\left(\frac{2}{\Delta t}+\frac{1}{\mathrm{Re}\Delta r^2}+\frac{1}{2\mathrm{Re}r^2_{i,j}}+\frac{1}{\mathrm{Re}\Delta z^2}\right)u^*_{i,j}+\left(\frac{w^n_{i,j}}{2\Delta z}-\frac{1}{2\mathrm{Re}\Delta z^2}\right)u^*_{i,j+1}=\frac{2u^n_{i,j}}{\Delta t}+\frac{p^*_{i-1,j}-p^*_{i+1,j}}{2\Delta r}+\left(\frac{u^n_{i,j}}{2\Delta r}+\frac{1}{2\mathrm{Re}\Delta r^2}-\frac{1}{4\mathrm{Re}r_{i,j}\Delta r}\right)u^*_{i-1,j}+\left(-\frac{u^n_{i,j}}{2\Delta r}+\frac{1}{2\mathrm{Re}\Delta r^2}+\frac{1}{4\mathrm{Re}r_{i,j}\Delta r}\right)u^*_{i+1,j}. \quad (15\text{-}3)$$

At each time level, the procedure iterates until the results of the velocity converge to the stable values with the accuracy up to the sixth decimal place. The same procedure is repeated for the next time step and the problem solution continues to a value of τ, where the results show a steady-state behavior. To investigate the independency of the grid size, several various step sizes are employed. The results are tabulated in Table 1 for $\mathrm{Re} = 1$, $\mathrm{Pr} = 1$, $\mathrm{Gr} = 0$, $R_{max} = 4$, and $Z_{min,max} = \pm 3$. The values of the velocity and temperature field are very close for all the step sizes listed in Table 1. Therefore, a comparison is made between inlet and outlet flow rates of the solution domain. The best choice of grid size would be $\Delta r = \Delta z = 0.05$; no convergence with our expected accuracy would occur for the values less than 0.02 due to truncation errors accumulation.

When the numerical solution is completed, the velocity and temperature field are known, and the values of Nusselt number, wall shear-stress, and entropy generation number can be determined numerically by Eqs. (10) and (12) to (14).

4. Results and discussions

The presented results by Gorla [3] are used to validate our computational code in the case of steady-state flow on a constant-wall-temperature cylinder. The

comparison of dimensionless function f with the same parameters of Re = 1, Pr = 1 and no buoyancy effects (Gr = 0) is shown in Figure 4. Note that dimensionless function f is equal to $[-r\ u]$, employed by Gorla in his similarity solution. In addition, the comparison of dimensionless temperature θ with different $R_{\max}$ is shown in Figure 5. in these two figures with respect to different values of $R_{\max}$ are obtained, whereas the values of $Z_{\min}$ and $Z_{\max}$ are fixed and equal to -3 and $+3$, respectively. It is observed that the results of the numerical solution and the similarity one are very close, which holds especially for small r, but does not match exactly because the similarity solution is actually a consequence of asymptotic situation $R_{\max} \to \infty$. In addition, by choosing greater values of $R_{\max}$, we would not find the results necessarily closer to the similar solution. So, the minimum difference between our results and Gorla's can be seen for $R_{\max} = 6$ and $R_{\max} = 7$ for two functions f and θ, respectively.

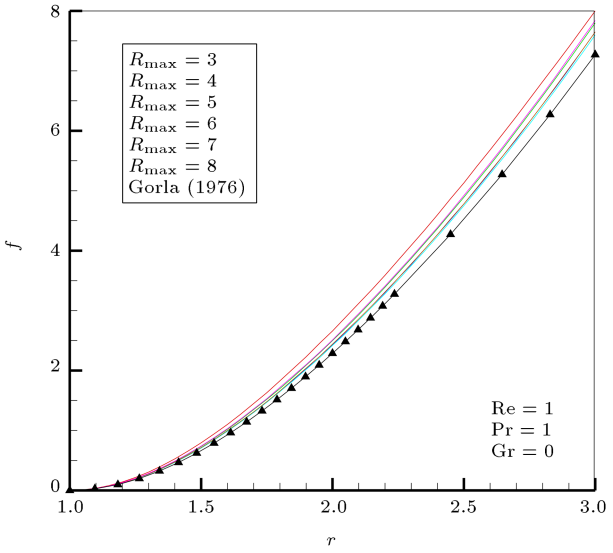

Figure 4. Distribution of the steady-state radial velocity function f at $z = 3/4$ for Re = 1, Pr = 1, Gr = 0 and $Z_{\min,\max} = \pm 3$ with different values of $R_{\max}$.

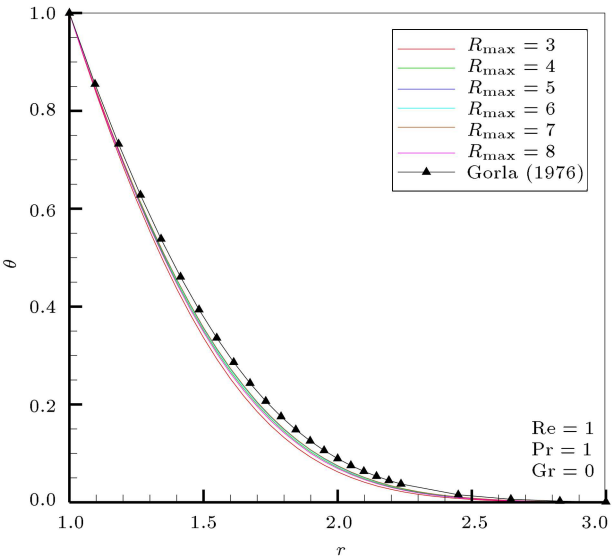

Figure 5. Distribution of the steady-state thermal function $\theta(r, z = 3/4)$ for Re = 1, Pr = 1, Gr = 0 and $Z_{\min,\max} = \pm 3$ with different values of $R_{\max}$.

Now, consider the case of the steady-state stagnation-flow equation on a cylinder with constant wall temperature, Pr = 0.7, and no gravity (Gr = 0). We conducted our computations in a solution domain with dimensions $R_{\max} = 3$ and $Z_{\max,\min} = \pm 3$ for three different Reynolds numbers. Distribution of the axial velocity (w/W) and thermal function, θ, against r at the specific value of $z = 3/4$ are shown in Figures 6 and 7. Moreover, the results of the Nusselt number and the dimensionless shear-stress on the cylinder's wall, τ_w, are plotted in Figures 8 and 9. According to Figure 6, at higher Reynolds numbers, the boundary

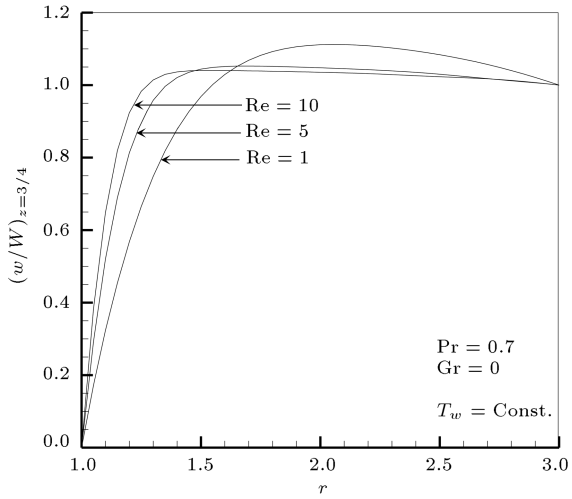

Figure 6. Distribution of axial velocity $w(r, z)$ against r for Re = 1, 5, 10.

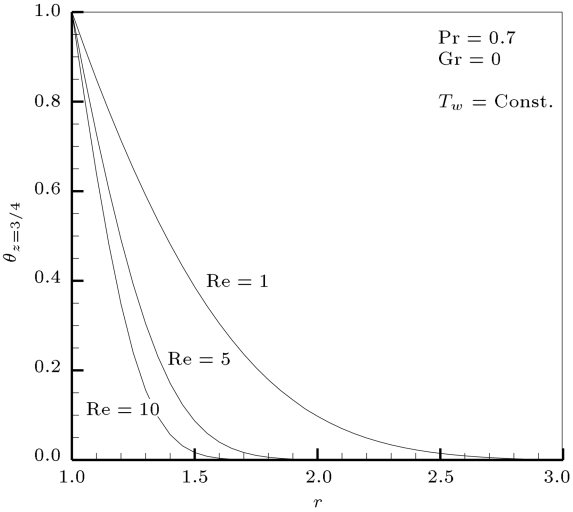

Figure 7. Distribution of thermal function $\theta(r, z)$ against r for Re = 1, 5, 10.

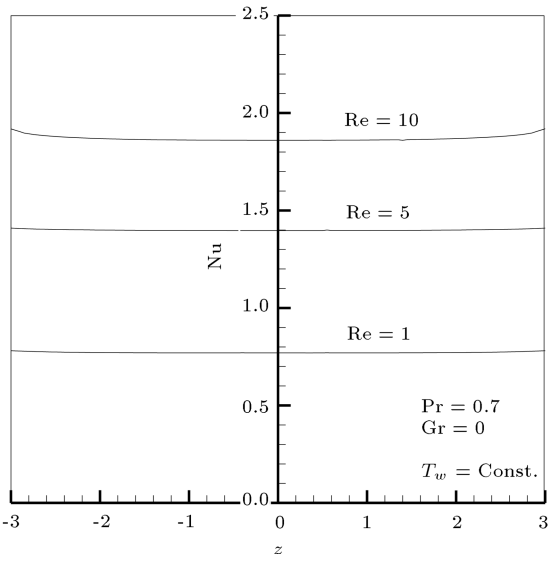

Figure 8. Variation of the Nusselt number against z for Re $= 1, 5, 10$.

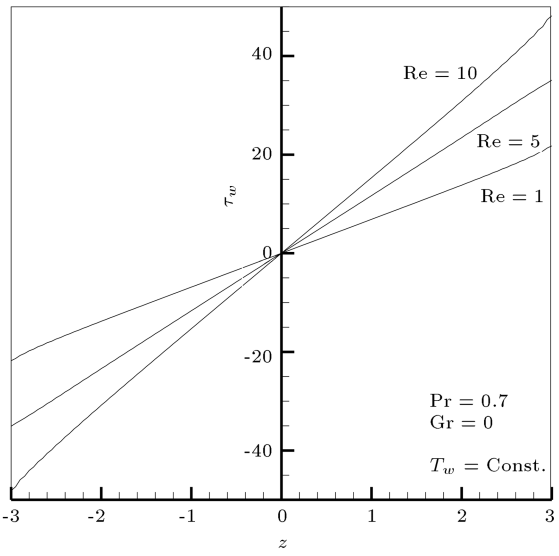

Figure 9. Variation of wall shear stress, τ_w, against z for Re $= 1, 5, 10$.

layer contracts toward the cylinder's wall. As can be seen, for Re=10, there is an intensive gradient of axial velocity (w/W) until about $r = 1.4$, which denotes the boundary layer region and, for Re $= 5$, it exists until $r = 1.6$. After that, we see a smooth variation in the velocity diagram, which is related to the outside region of the boundary layer. However, for Re $= 1$, these two regions are not clearly distinguishable, and it is better to use a calculation domain with larger dimension, $R_{\max}$, for this low Reynolds number. According to Figure 7, the thermal boundary layer for Re $= 1$, 5, and 10 expands to $r = 2.7$, 1.8, and 1.6, approximately. Our calculation shows that the value of $R_{\max}$ does not have considerable effects on these diagrams. This is because the variation of the flow temperature against

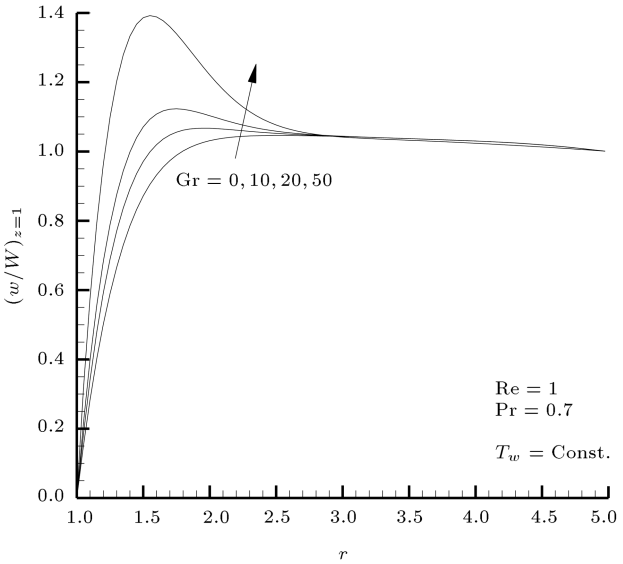

Figure 10. Distribution of axial velocity $w(r, z = 1)$ against r for Gr $= 0$, 10, 20, 50 when the cylinder's wall temperature is constant (T_w = Const.).

r is highly affected by velocity u, and this velocity component does not change much with the dimension of the solution domain. According to Figure 8, the value of the Nusselt number is constant along the cylinder's axis, as expected. Only near the boundaries, we witness a slight variation in Nu which is due to our approximation of the boundary conditions (Eq. (9)). Through ignoring this insignificant error, for Re $= 1$, 5, and 10, the average values of the Nusselt number are 0.77, 1.4, and 1.86, respectively. It can clearly be seen from Figure 9 that the shear-stress on the cylinder's surface has a linear variation along the axis. Since Gr $= 0$, the flow is symmetric against line $z = 0$ and, so, $\tau_w = 0$ (stagnation-point) occurs exactly at $z = 0$, too.

For other cases of the problem, the flow with constant parameters, Re=1 and Pr $= 0.7$, yet with variable Grashof numbers, is considered. Herein, the dimensions of the domain of solution as $R_{\max} = 5$ and $Z_{\max,\min} = \pm 4$ are chosen, which are appropriate for Re $= 1$. The resulting diagrams in Figures 10 to 14 are related to the flow characteristics in the steady state when the temperature of the cylinder's wall is constant and Grashof number has a constant value, as well. These diagrams are presented for Gr $= 0$, 5, 10, 20, and 50. In Figure 10, the assisting effect of the buoyancy forces in the distribution of velocity, w, is observed. This effect causes the velocity to grow; for example, for Gr $= 50$, this growth is about 1.5 times the case of no-buoyancy condition. In contrast, the opposing effect of the buoyancy forces, which is shown in Figure 11 for $z = -1$, causes velocity, w, to decrease to zero and even reverse its value (as it occurs for Gr $= 50$). According to Figure 12, distribution of temperature has a very slight variation against the large variation of

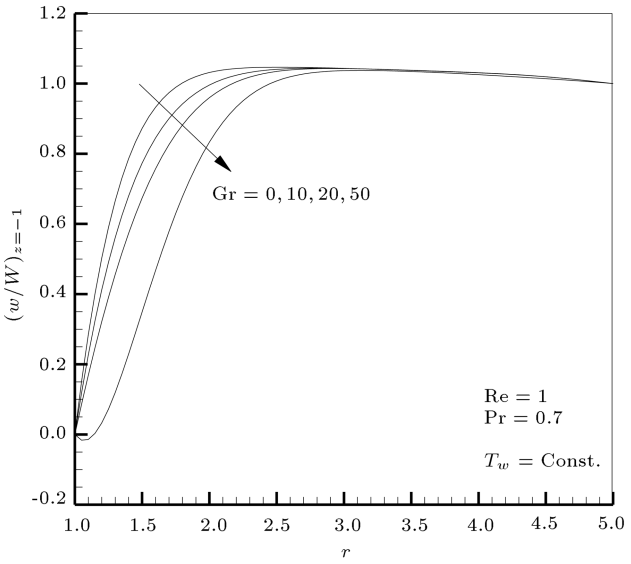

Figure 11. Distribution of axial velocity $w(r, z = -1)$ against r for Gr = 0, 10, 20, 50 when the cylinder's wall temperature is constant (T_w = Const.).

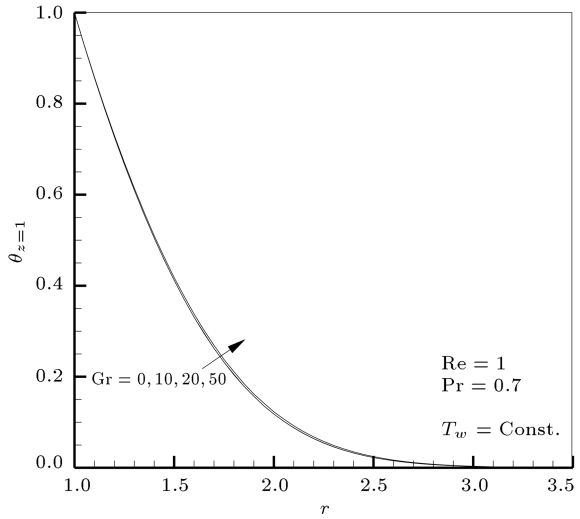

Figure 12. Distribution of the thermal function $\theta(r, z)$ against r for Gr = 0, 10, 20, 50 when the cylinder's wall temperature is constant (T_w = Const.).

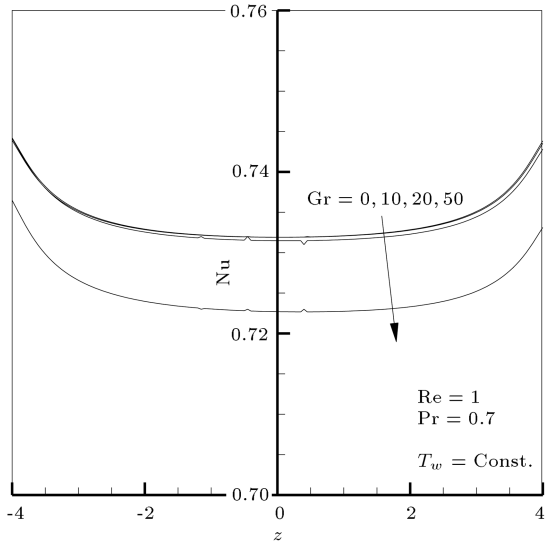

Figure 13. Variation of the Nusselt number against z for Gr = 0, 10, 20, 50 when the cylinder's wall temperature is constant (T_w = Const.).

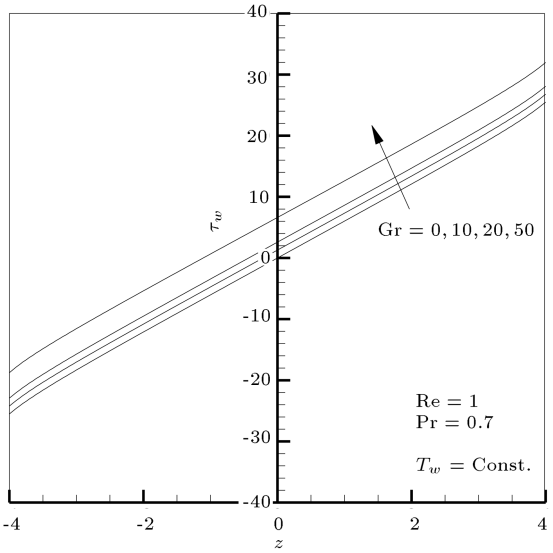

Figure 14. Variation of wall shear-stress T_w against z for Gr = 0, 10, 20, 50 when the cylinder's wall temperature is constant (T_w = Const.).

Grashof numbers. Similarly, this situation exists for Nusselt number (Figure 13). Thus, there exist 0.732, 0.732, 0.731, and 0.723 for Nusselt number at the center against Gr = 0, 10, 20, and 50, respectively. By referring to Figure 14, for this case of wall temperature (T_w = const.) and for larger Grashof numbers, it is seen that the shear stress along the surface increases uniformly. The existence of buoyancy forces moves the stagnation-point (the position of $\tau_w = 0$) downward. For instance, at Gr = 20, the stagnation-point is located at $z = -0.43$. The flow streamlines for the two cases of Gr = 0 and Gr = 50 are illustrated in Figure 15. From this figure, the effects of the buoyancy forces and, consequently, the streamlines deformation near the wall are clearly visible for Gr = 50, as well as downward movement of the stagnation-point.

When the cylinder's wall temperature varies linearly against z and is symmetrical about $z = 0$, it can be expressed as $T_w - T_\infty = |b\ z|$ in which b is a constant coefficient. Therefore, Grashof number, according to its definition by Eq. (7), varies linearly against z. Obviously, the following are inserted into Eq. (6):

$$\frac{\frac{dT_w}{dz}}{T_w - T_\infty} = \frac{1}{z}, \qquad \frac{d^2 T_w}{dz^2} = 0. \tag{16}$$

The results of the problem under this condition with

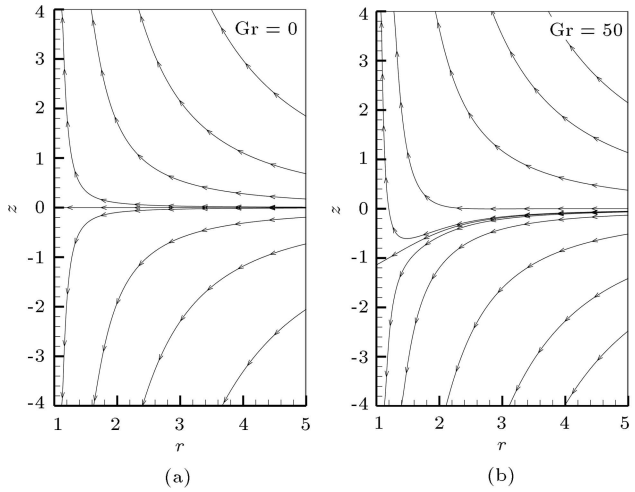

Figure 15. Illustration of the flow streamlines for Re = 1, Pr = 0.7, and T_w = Const.: (a) Gr = 0, and (b) Gr = 50.

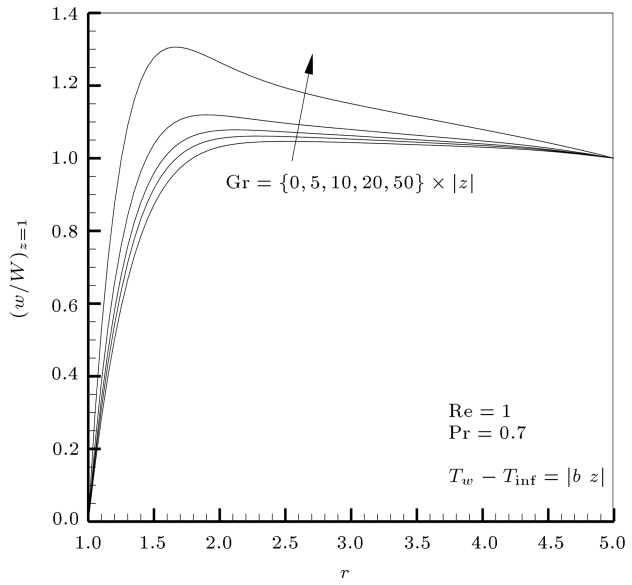

Figure 16. Distribution of axial velocity $w(r, z = 1)$ against r for Gr = 0, $10z$, $20z$, $50z$ when the cylinder's wall temperature varies linearly ($T_w = |b\ z|$).

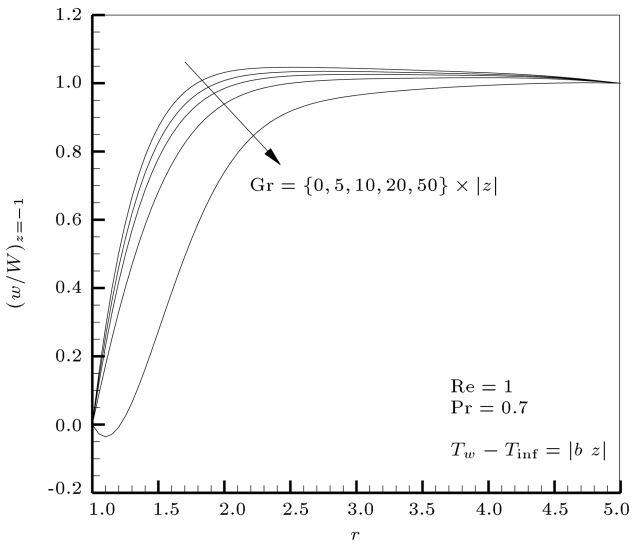

Figure 17. Distribution of axial velocity $w(r, z = -1)$ against r for Gr = 0, $10z$, $20z$, $50z$ when the cylinder's wall temperature varies linearly ($T_w = |b\ z|$).

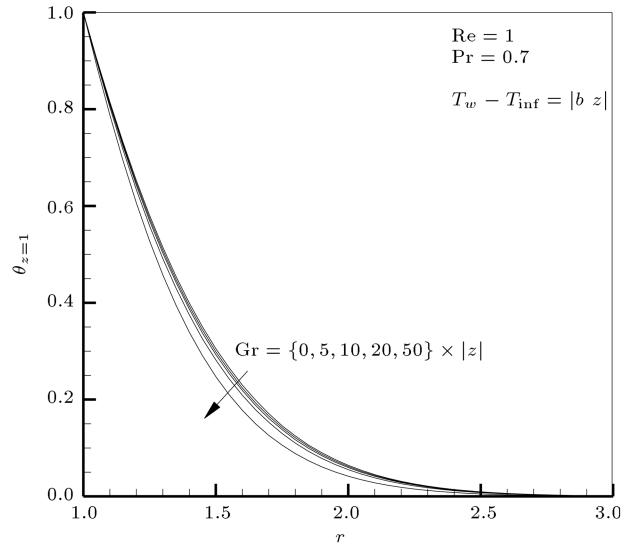

Figure 18. Distribution of thermal function $\theta(r, z)$ against r for Gr = 0, $10z$, $20z$, $50z$ when the cylinder's wall temperature varies linearly ($T_w = |b\ z|$).

$Gr = 0$, $|5z|$, $|10z|$, $|20z|$, and $|50z|$, which are plotted for the steady-state case, are depicted in Figures 16 to 20. In Figure 19, the diagrams of Nusselt number take apart at $z = 0$ with each part tending towards infinity because this point is a singular point ($T_w - T_\infty = 0$). For $z > 0$, Nusselt number has greater values compared to the case of Gr = 0 and for $z < 0$ in which its values are less. Also, variations of τ_w for Gr = 0, 5, 10, 20, and 50 are presented in Figure 20. At high Grashof numbers, the variation seems to be nonlinear and the diagram takes a convexity, especially near the outlet boundaries.

For the final case, it is supposed that the temperature of the cylinder has a parabolic variation against z. Herein, the temperature profile is as $T_w - T_\infty = bz^2$ with b as a constant coefficient; consequently:

$$\frac{\frac{d_w}{dz}}{T_w - T_\infty} = \frac{2}{z}, \qquad \frac{\frac{d^2 T_w}{dz^2}}{T_w - T_\infty} = \frac{2}{z^2}. \tag{17}$$

Since the Grashof number has the same parabolic variation, sample states Gr = 0, $5z^2$, $10z^2$ were considered to perform our calculation. The results are illustrated in Figures 21 to 25 under the steady-state condition. According to Figure 24, Nusselt number near $z = 0$ tends toward the negative infinity rapidly. This result is unlike what happened in the previous case in Figure 19. The variation of shear-stress, τ_w, shown in Figure 25, has more nonlinearity than that of

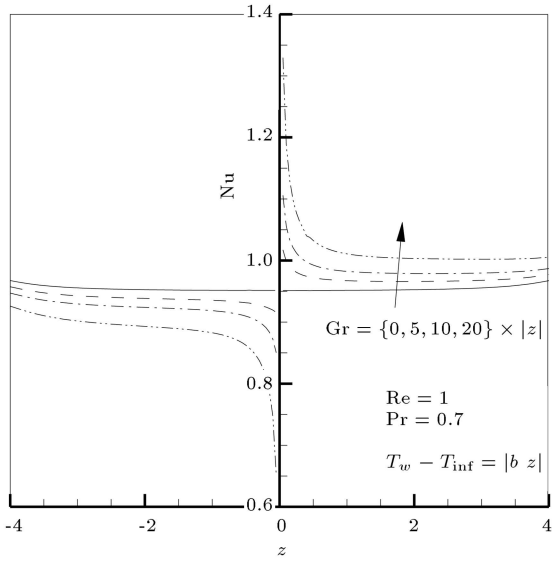

Figure 19. Variation of the Nusselt number against z for Gr = 0, $10z$, $20z$, $50z$ when the cylinder's wall temperature varies linearly ($T_w = |b\ z|$).

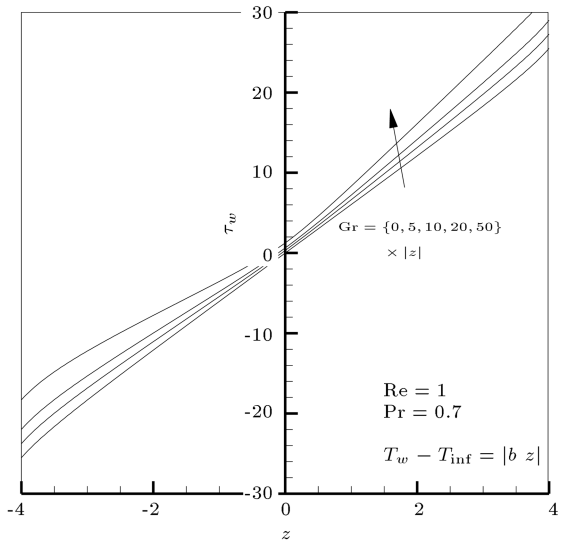

Figure 20. Variation of wall shear stress τ_w against z for Gr = 0, $10z$, $20z$, $50z$ when the cylinder's wall temperature varies linearly ($T_w = |b\ z|$).

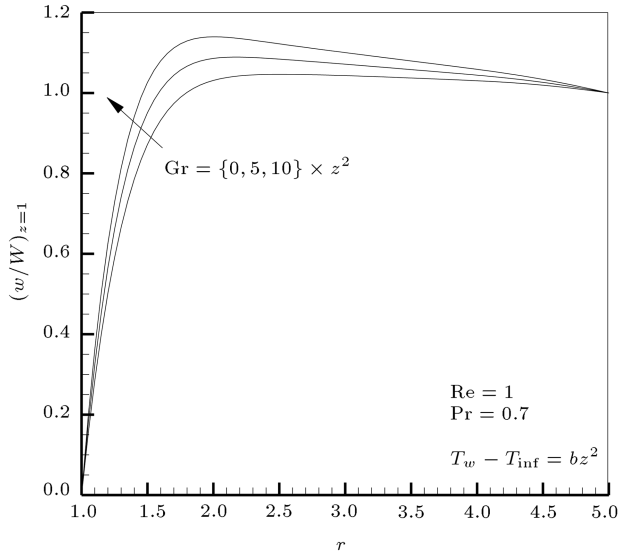

Figure 21. Distribution of axial velocity $w(r, z = 1)$ against r for Gr = 0, $5z^2$, $10z^2$ when the cylinder's wall temperature varies parabolic ($T_w = bz^2$).

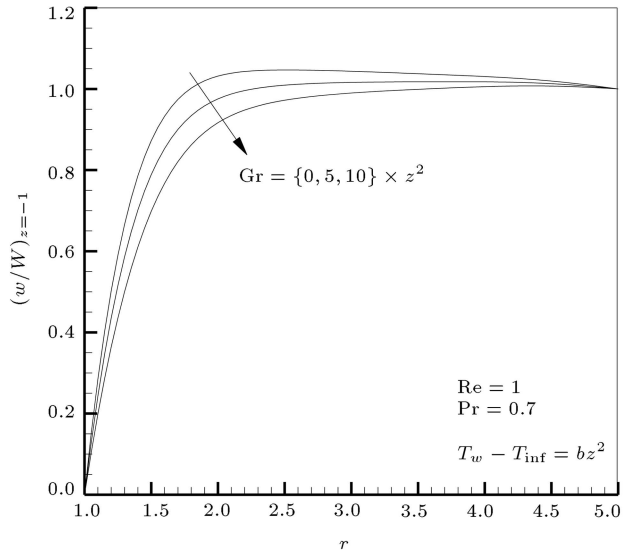

Figure 22. Distribution of axial velocity $w(r, z = -1)$ against r for Gr = 0, $5z^2$, $10z^2$ when the cylinder's wall temperature varies parabolic ($T_w = bz^2$).

the previous case. Time-dependent variations of two parameters τ_w and Nu are illustrated in Figures 26 and 27 in the case of T_w = const. at $z = 0.5$. As observed, τ_w experiences an unstable variation along time parameter τ, until it comes close to the steady-state condition. In addition, a sudden change in the diagrams appears at about $\tau = 0.1$. Herein, the results of the numerical computation transfer from the initial inviscid values to the viscous results are shown. After that, due to gradual balancing of the pressure field over the computation domain, the results are subject to instability, disappearing over time. The variations of the Nusselt number were plotted for three sample Prandtl numbers. At the first instants of time, the Nusselt numbers are almost the same regardless of the value of Pr; however, with the passage of time, it drops rapidly. This sudden drop is more severe for smaller Prandtl numbers, which finally leads to a smaller Nu in the steady-state case. Thus, in the steady-state case, we will have Nu = 0.7, 1.5, and 3.7 for Pr = 0.7, 7, and 70, respectively. As known, the smaller the Prandtl number, the higher the thermal diffusivity, which causes the conduction heat transfer mechanism to dominate compared to convection heat transfer; hence, smaller Nusselt number is produced.

Finally, an entropy generation analysis was ap-

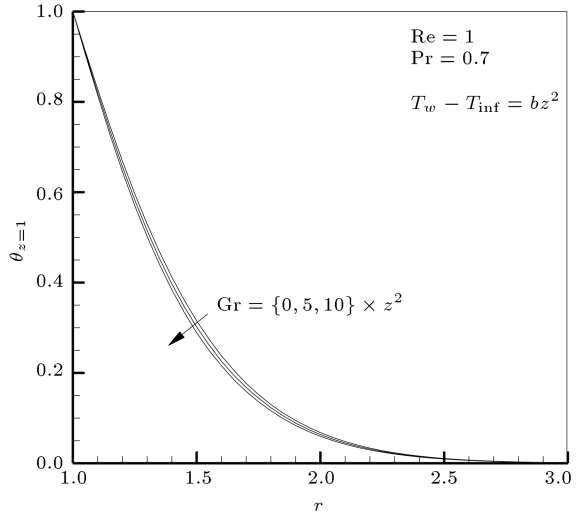

Figure 23. Distribution of thermal function $\theta(r, z)$ against r for Gr $= 0$, $5z^2$, $10z^2$ when the cylinder's wall temperature varies parabolic ($T_w = bz^2$).

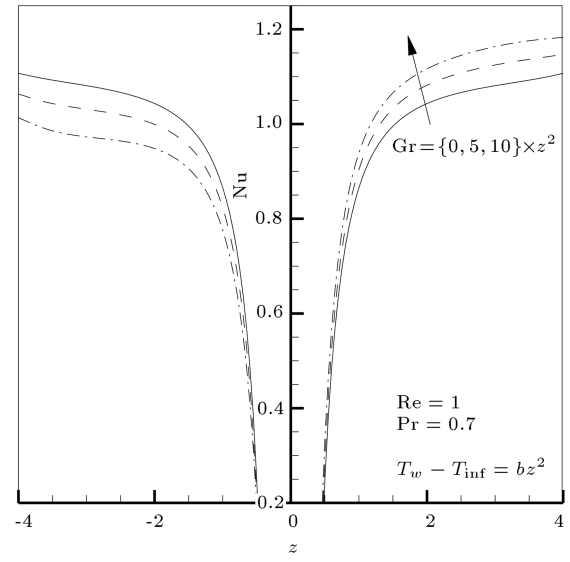

Figure 24. Variation of the Nusselt number against z for Gr $= 0$, $5z^2$, $10z^2$ when the cylinder's wall temperature varies parabolic ($T_w = bz^2$).

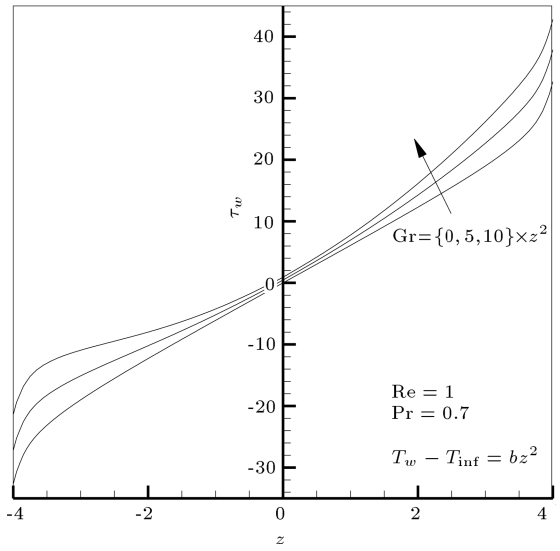

Figure 25. Variation of wall shear-stress τ_w against z for Gr $= 0$, $5z^2$, $10z^2$ when the cylinder's wall temperature varies parabolic ($T_w = bz^2$).

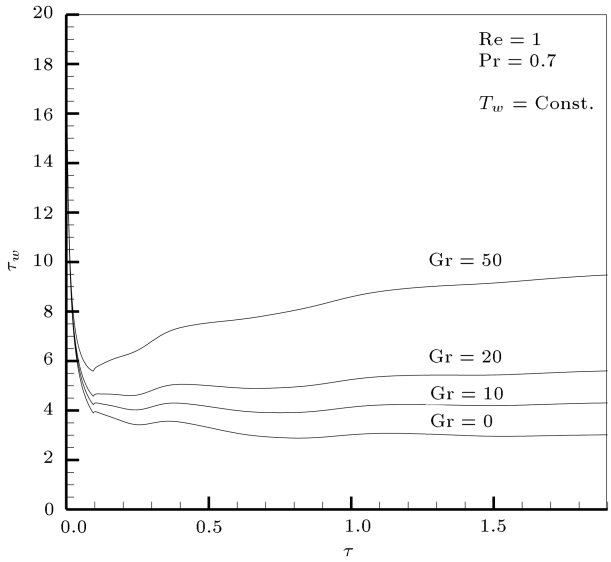

Figure 26. Variation of wall shear-stress τ_w at $z = 0.5$ against time parameter τ for Gr $= 0$, 10, 20, 50 with Re $= 1$ and Pr $= 0.7$.

plied to the sample case of Re $= 1$, Pr $= 0.7$, Br $= 1$, and $T_w =$ Const. The results are shown in Figure 28 for Gr $= 0$ (no free convection) and Figure 29 for a constant ratio of T_w/T_∞ ($\gamma = 1.2$). According to Figure 28, when the ratio of T_w to T_∞ increases, both N_s and Be increase significantly, even though their difference is a constant, which is due to the role of absolute temperature in entropy production mechanism. On the other hand, according to Figure 29, when the ratio of T_w/T_∞ is a constant, the existence of free convection heat transfer can exert an increasing effect on N_s in the region of boundary layer flow. However, Be number can vary from 0 to 1; however, in the present problem, its value does not exceed 0.1 even for large γ. This is because of the outer flow, which has a significant share in entropy generation by viscous losses. This means that almost all of the entropy generations are the result of fluid flow and not the heat transfer.

5. Conclusions

The unsteady problem of mixed convection heat transfer from a vertical cylinder impinged by an impulsive axisymmetric stagnation-point flow was solved, numerically. A computational code, provided by the authors based on SIMPLE algorithm, was employed to predict

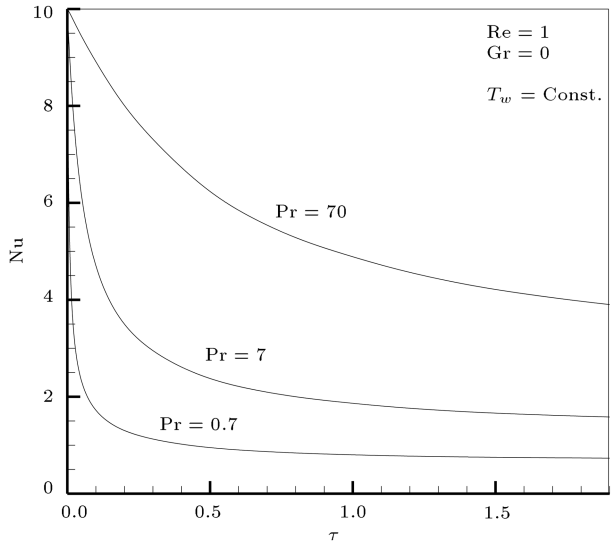

Figure 27. Variation of the Nusselt number at $z = 0.5$ against time parameter τ for Pr = 0.7, 7, 70 with Re = 1 and Gr = 0.

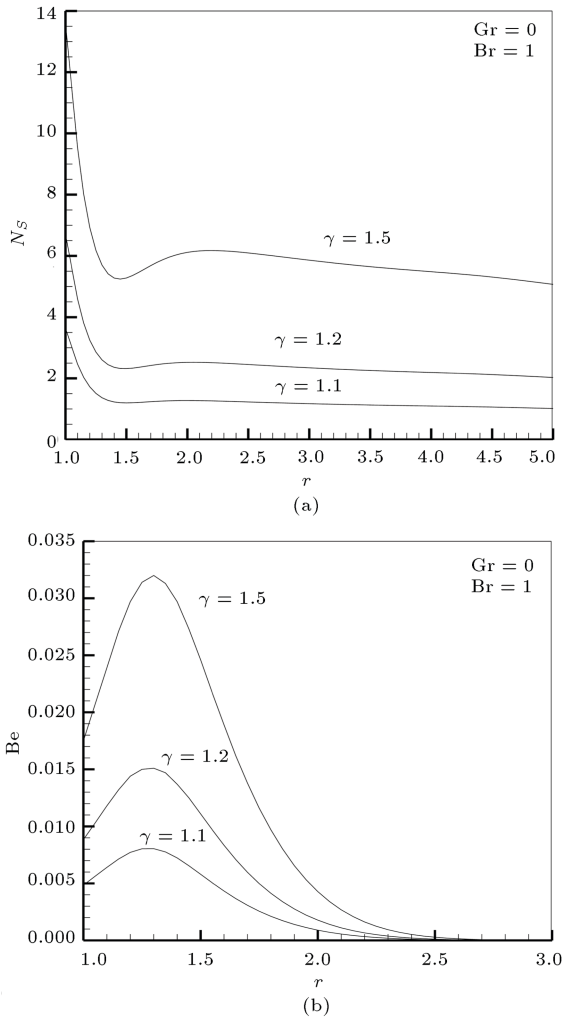

Figure 28. Effect of temperature ratio γ on (a) entropy generation number and (b) Be number at $z = 1$ for Re = 1, Pr = 0.7, Gr = 0, Br = 1, and T_w = Const.

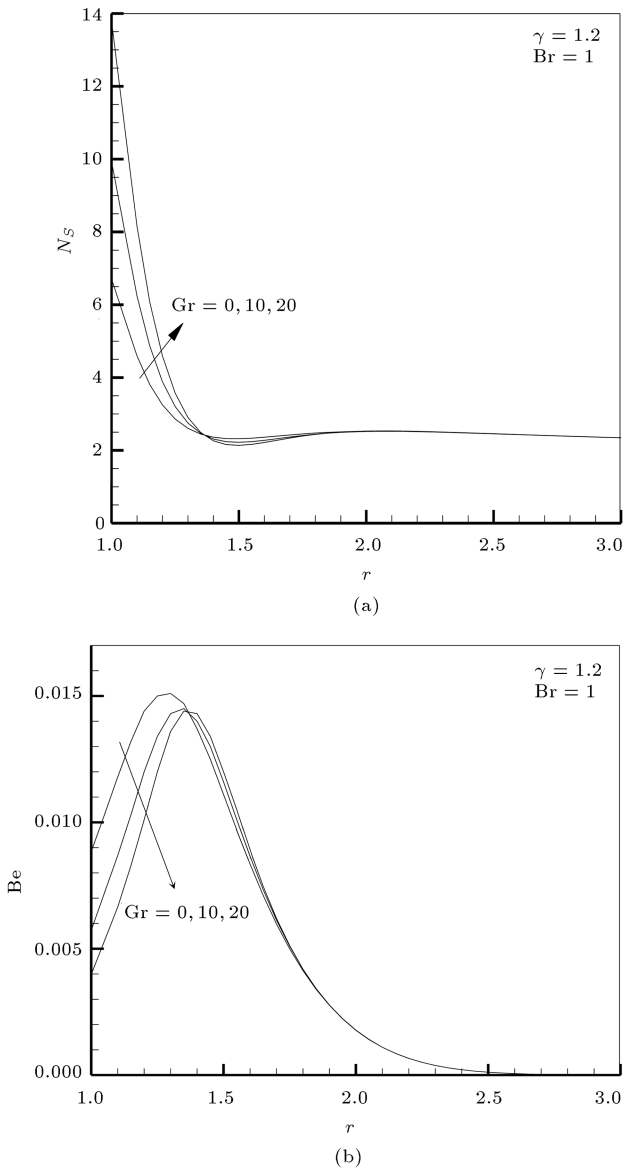

Figure 29. Effect of Gr number on (a) entropy generation number and (b) Be number at $z = 1$ for Re = 1, Pr = 0.7, γ = 1.2, Br = 1 and T_w = Const.

the buoyancy effects of different distributions of the cylinder's wall temperature on the flow characteristics. For outer flow, which is supposed to be inviscid, simple analytical equations govern; however, in the domain of solution where flow has a viscous behavior, Navier-Stokes and energy equations were discretized and the resulting 3-equation system was solved by an implicit finite-difference method. The steady-state result was comparable to that formerly obtained by similarity solutions. The distribution of velocity components u and w against r shows that the numerical results of the problem would be close to the similarity ones by choosing appropriate size of $R_{\max}$ for the domain of solution. The numerical method, presented here, derives its importance from the shortcomings of similarity

method in solving all types of the problems. Therefore, in the present paper, after validation of the numerical method, it solved the time-dependent problem in three various distributions of the cylinder's wall temperature (constant, linear, and parabolic distributions) at some different Grashof numbers. The results of the velocity and temperature showed almost similar distributions for the mentioned cases of the problem; however, the variations of the wall shear-stress and Nusselt number along the cylinder's axis were completely different in each case. When the cylinder's wall temperature has a linear or parabolic form, $\tau_w - z$ diagram does not have a linear form yet, also $\mathrm{Nu} - z$ diagram possessed a singular point at $z = 0$ and divided the domain into two separated parts for $z < 0$ and $z > 0$. In this problem, the entropy generation analysis shows that viscous irreversibility effects play the main role leading to very low Be numbers.

Nomenclature

a	Cylinder radius (m)
b	Constant coefficient (K)
Be	Bejan number
Br	Brinkman number
Gr	Grashof number
f	Dimensionless velocity function
g	Gravitational acceleration (m/s^2)
h	Convective heat transfer coefficient ($W/m^2.K$)
k	Thermal conductivity (W/m.K)
$\bar{k}$	Strength of the free stream flow (1/s)
N_F	Entropy generation number, fluid friction
N_H	Entropy generation number, heat transfer
N_S	Entropy generation number, overall
Nu	Nusselt number
p	Dynamic pressure (Pa)
Pr	Prandtl number
r	Dimensionless coordinate in radial direction of cylinder
$R_{\max}$	Position of the solution domain's boundary in r-direction
Re	Reynolds number
$\dot{S}'''_{\mathrm{gen}}$	Volumetric entropy generation rate (W/m^3K)
u, w	Dimensionless viscous flow's r and z-component of velocity
U, W	Dimensionless invicsid flow's r and z-component of velocity
z	Dimensionless coordinate in axial direction of cylinder
t	Time (s)
T	Temperature (K)
T_w	Temperature on the cylinder's wall (K)
T_∞	Free stream temperature (K)
$Z_{\max}$	Upper limit of the solution domain's boundary in z-direction
$Z_{\min}$	Lower limit of the solution domain's boundary in z-direction
α	Thermal diffusivity (m^2/s)
β	Volumetric thermal expansion coefficient (1/K)
θ	Dimensionless temperature
μ	Dynamic viscosity (Pa.s)
ν	Kinematics viscosity (m^2/s)
ρ	Density (m^3)
τ	Dimensionless time
τ_w	Dimensionless shear stress on the cylinder's wall
γ	Temperature ratio
Φ	Viscous dissipation function (W/m^3)

References

1. Hiemenz, K. "Axisymmetric stagnation-point flow on a cylinder" [Die Grenzchicht an einem in den gleichformingen Flussigkeitsstrom eingetauchten graden Kreiszylinder], *Dinglers Polytech. J.*, **236**, pp. 321-410 (1911).
2. Wang, C. "Axisymmetric stagnation flow on a cylinder", *Quarterly of Applied Mathematics*, **10**, pp. 207-213 (1974).
3. Gorla, R.S.R. "Heat transfer in an axisymmetric stagnation flow on a cylinder", *Applied Scientific Research*, **32**(5), pp. 541-553 (1976).
4. Gorla, R.S.R. "Transient response behavior of an axisymmetric stagnation flow on a circular cylinder due to time dependent free stream velocity", *International Journal of Engineering Science*, **16**(7), pp. 493-502 (1978).
5. Gorla, R.S.R. "Unsteady viscous flow in the vicinity of an axisymmetric stagnation point on a circular cylinder", *International Journal of Engineering Science*, **17**(1), pp. 87-93 (1979).
6. Ramachandran, R., Chen, T.S., and Armaly, B.F. "Mixed convection in stagnation flows adjacent to vertical surfaces", *ASME J. Heat Transf.*, **110**, pp. 373-377 (1988).
7. Gorla, R. "Mixed convection in an axisymmetric stagnation flow on a vertical cylinder", *Acta Mechanica*, **99**(1-4), pp. 113-123 (1993).

8. Takhar, H., Chamkha, A., and Nath, G. "Unsteady axisymmetric stagnation-point flow of a viscous fluid on a cylinder", *International Journal of Engineering Science*, **37**(15), pp. 1943-1957 (1999).
9. Rahimi, A. "Heat transfer in an axisymmetric stagnation flow at high Reynolds numbers on a cylinder using perturbation techniques", *Scientia Iranica*, **10**(1), pp. 116-121 (2003).
10. Saleh, R. and Rahimi, A.B. "Axisymmetric stagnation point flow of a viscous fluid on a moving cylinder with time dependent axial velocity", *International Journal of Engineering*, **17**(1), p. 8 (2004).
11. Saleh, R. and Rahimi, A. "Axisymmetric stagnation-point flow and heat transfer of a viscous fluid on a moving cylinder with time-dependent axial velocity and uniform transpiration", *Journal of Fluids Engineering*, **126**(6), pp. 997-1005 (2004).
12. Saleh, R. and Rahimi, A. "Axisymmetric radial stagnation-point flow of a viscous fluid on a rotating cylinder with time-dependent angular velocity", *Scientia Iranica*, **12**(4), pp. 329-337 (2005).
13. Rahimi, A.B. and Saleh, R. "Axisymmetric stagnation point flow and heat transfer of a viscous fluid on a rotating cylinder with time dependent angular velocity", *Journal of Fluids Engineering*, **129**, pp. 106-115 (Jan. 2007).
14. Rahimi, A. and Saleh, R. "Unaxisymmetric heat transfer in the axisymmetric Stagnation point flow of a viscous fluid on a cylinder with simultaneous axial and rotational movement along with transpiration", *Scientia Iranica*, **15**(3), pp. 366-377 (2008).
15. Revnic, C., Grosan, T., Merkin, J., and Pop, I. "Mixed convection flow near an axisymmetric stagnation point on a vertical cylinder", *Journal of Engineering Mathematics*, **64**(1), pp. 1-13 (2009).
16. Mohammadiun, H. and Rahimi, A.B. "Stagnation-point flow and heat transfer of a viscous, compressible fluid on a cylinder", *Journal of Thermophysics and Heat Transfer*, **26**(3), pp. 494-502 (2012).
17. Lok, Y.Y., Merkin, J.H., and Pop, I. "Mixed convection flow near the axisymmetric stagnation point on a stretching or shrinking cylinder", *International Journal of Thermal Sciences*, **59**, pp. 186-194 (2012).
18. Mohammadiun, H., Rahimi, A.B., and Kianifar, A. "Axisymmetric stagnation-point flow and heat transfer of a viscous, compressible fluid on a cylinder with constant heat flux", *Scientia Iranica*, **20**(1), pp. 185-194 (2013).
19. Bayat, R. and Rahimi, A.B. "Unsteady impulsive oblique stagnation-point flow impinging axisymmetrically on a vertical circular cylinder with mixed convection heat transfer", *Scientia Iranica*, **24**(4), pp. 1966-1974 (2017).
20. Bejan, A., *Entropy Generation Through Heat and Fluid Flow*, New York, Wiley (1994).

Biographies

Reza Bayat was born in Mashhad, Iran in 1977. He received his BS degree in Mechanical Engineering from Ferdowsi University of Mashhad in 1999 and his MS degree in Mechanical Engineering from Sharif University of Technology in Mechanical Engineering in 2001. He is currently a PhD candidate in Ferdowsi University of Mashhad.

Asghar Baradaran Rahimi was born in Mashhad, Iran in 1951. He received his BS degree in Mechanical Engineering from Tehran polytechnic, in 1974, and a PhD degree in Mechanical Engineering from the University of Akron, Ohio, USA in 1986. He has been a Professor at the Department of Mechanical Engineering in Ferdowsi University of Mashhad since 2001. His research and teaching interests include heat transfer and fluid dynamics, gas dynamics, continuum mechanics, applied mathematics, and singular perturbations.